Published in final edited form as:
J Autoimmun. 2013 August ; 44: 21–33. doi:10.1016/j.jaut.2013.06.003.

Breakdown of immune privilege and spontaneous autoimmunity in mice expressing a transgenic T cell receptor specific for a retinal autoantigen

Reiko Horai[a,*], **Phyllis B. Silver**[a,5], **Jun Chen**[a,5], **Rajeev K. Agarwal**[a,1,5], **Wai Po Chong**[a], **Yingyos Jittayasothorn**[a], **Mary J. Mattapallil**[a], **Sonia Nguyen**[a], **Kannan Natarajan**[b], **Rafael Villasmil**[c], **Peng Wang**[a,2], **Zaruhi Karabekian**[a,3], **Simon D. Lytton**[a,4], **Chi-Chao Chan**[a], and **Rachel R. Caspi**[a,*]

[a]Laboratory of Immunology, National Eye Institute, National Institutes of Health, Bethesda, MD 20892-1857, USA

[b]Laboratory of Immunology, National Institute of Allergy and Infectious Diseases, National Institutes of Health, Bethesda, MD, USA

[c]Flow Cytometry Core, National Eye Institute, National Institutes of Health, Bethesda, MD, USA

Abstract

Despite presence of circulating retina-specific T cells in healthy individuals, ocular immune privilege usually averts development of autoimmune uveitis. To study the breakdown of immune privilege and development of disease, we generated transgenic (Tg) mice that express a T cell receptor (TCR) specific for interphotoreceptor retinoid-binding protein (IRBP), which serves as an autoimmune target in uveitis induced by immunization. Three lines of TCR Tg mice, with different levels of expression of the transgenic R161 TCR and different proportions of IRBP-specific $CD4^+$ T cells in their peripheral repertoire, were successfully established. Importantly, two of the lines rapidly developed spontaneous uveitis, reaching 100% incidence by 2 and 3 months of age, respectively, whereas the third appeared “poised” and only developed appreciable disease upon immune perturbation. Susceptibility roughly paralleled expression of the R161 TCR. In all three lines, peripheral $CD4^+$ T cells displayed a naïve phenotype, but proliferated *in vitro* in response to IRBP and elicited uveitis upon adoptive transfer. In contrast, $CD4^+$ T cells infiltrating uveitic eyes mostly showed an effector/memory phenotype, and included Th1, Th17 as well as T regulatory cells that appeared to have been peripherally converted from conventional $CD4^+$ T cells rather than thymically derived. Thus, R161 mice provide a new and valuable model of spontaneous autoimmune disease that circumvents the limitations of active immunization and adjuvants, and allows to study basic mechanisms involved in maintenance and breakdown of immune homeostasis affecting immunologically privileged sites such as the eye.

Keywords

Autoimmune uveitis; Immune privilege; TCR transgenic mouse; Spontaneous disease

[*]Corresponding authors. Tel.: +1 301 435 4555, +1 301 435 4573. hreiko@mail.nih.gov (R. Horai), caspir@mail.nih.gov, rcaspi@helix.nih.gov (R.R. Caspi). .
[1]Present address: Translational Research Program, Division of Cancer Treatment and Diagnosis, National Cancer Institute, National Institutes of Health, Rockville, MD, USA.
[2]Present address: Beijing Biobank of Clinical Resources, Capital Medical University, Beijing, China.
[3]Present address: The George Washington University, Washington DC, USA.
[4]Present address: SeraDiaLogistics, 81545 Munich, Germany.
[5]These authors contributed equally to this work.

1. Introduction

The healthy eye resides behind a protective blood-retinal barrier that prevents free movement of cells and even large molecules into and out of the globe. This sequestration of the eye from the immune system is part of the phenomenon known as immune privilege of the eye, which protects the delicate ocular structures that are critical to vision from collateral damage as a consequence of environmental inflammatory insults [1]. However, this separation from the immune system arguably also impedes efficient induction of peripheral tolerance to eye-specific antigens, allowing persistence in the circulation of non-tolerized eye-reactive T cells. This may help to explain why, despite immune privilege, the eye is subject to destructive autoimmunity manifesting as uveitis [2].

Uveitis is a group of blinding inflammatory diseases that result in destruction of the light-sensitive photoreceptor cells of the neuroretina [3]. Uveitic diseases are estimated to underlie 10–15% of legal blindness in the developed world [4,5]. In most cases of human uveitis the pathogenic trigger is unknown. A notable exception is sympathetic ophthalmia, in which a penetrating trauma to one eye is followed, weeks or months later, by a destructive inflammation in the uninjured, “sympathizing” eye. This can be facilitated by inflammation that often accompanies such an injury. Available evidence, including recall responses to eye-derived antigens often seen in such patients, led to the notion that normally sequestered antigens from the eye drain into the regional lymph node and elicit a systemic autoimmune response, which then precipitates the autoimmune attack on the uninjured eye. Many human patients exhibit responses to retinal arrestin (also known as the retinal soluble antigen, or S–Ag) and some respond to interphotoreceptor retinoid-binding protein (IRBP) and other retinal proteins [6-10].

Experimental autoimmune uveitis (EAU) induced in susceptible animal models by systemic immunization with retina-derived antigens or their peptides emulsified in complete Freund’s adjuvant (CFA) mimics this systemic autoimmunization response [11]. While in humans the major retinal antigen being recognized appears to be arrestin, mice preferentially develop uveitis with IRBP. The reason for this species-specific preference may be connected to the MHC and presentation of appropriate epitopes, as “humanized” HLA transgenic mice become susceptible to arrestin-induced EAU [12]. While immunization-induced EAU has been a valuable tool for modeling uveitis and the cellular mechanisms that drive it, the vast majority of uveitis cases present without evidence of trauma to the eye that could cause autoimmunization [3], and may not be adequately represented by this model. In addition, induction of EAU by immunization is dependent on massive stimulation of the immune system by the mycobacteria in CFA, which again may not be representative of human disease. We, therefore, set out to establish an alternative model of uveitis by generating mice transgenic for a retina-specific T cell receptor (TCR).

TCR Tg mice have been helpful in studying tissue-specific autopathogenic responses in other autoimmune diseases including models of type 1 diabetes, autoimmune gastritis and multiple sclerosis [13-21]. However, TCR Tg mice that respond to native retinal antigens have not been available to study ocular autoimmunity. Double-Tg mice, in which hen egg lysozyme (HEL) or β-galactosidase were expressed as retinal neo-self antigens under different retina-specific promoters, and combined with the corresponding TCR transgene, have yielded confusing results. Namely, levels of retinal and of thymic expression of the neo-self Ag, and most importantly, the ability of the transgenic host to develop uveitis were variable, and did not seem to be easily explained either by the identity of the retina-specific promoter or of the neo-Ag placed under its control [22-25].

Because the level and pattern of expression of neo-self antigens may vary, and may not mimic the endogenous Ag, we generated TCR Tg mice expressing a TCR specific to the endogenous uveitogenic antigen IRBP. Three lines expressing different levels of the same TCR displayed different susceptibilities to spontaneous disease, which could be correlated to transgene copy numbers and levels of peripheral expression of the transgenic TCR, for an analyzable effect on disease pathogenesis. These mice constitute the first model for a spontaneous uveitis directed at a native retinal Ag and promise to shed light on how T cells reactive to retina become primed and cause autoimmunity.

2. Materials and methods

2.1. Mice

B10.RIII mice were from Jackson Laboratory (B10.RIII-H2^{r} H2-T18^{b}/(71NS)SnJ). B10.A RAG2$^{-/-}$ mice were from Taconic Farms (Taconic Farms, Inc.), and were backcrossed to B10.RIII. IRBP TCR Tg (R161) mice were generated in house on the B10.RIII background (see ahead), and were maintained on the B10.RIII background or were crossed to B10.RIII RAG2$^{-/-}$ mice. All animals were maintained under specific pathogen free conditions. Animal care and use followed Institutional guidelines, animal study protocol #NEI-581.

2.2. Cloning of IRBP-specific TCR and generation of TCR Tg mice

TCR α and β chains were cloned from a highly uveitogenic T cell line specific to the IRBP$_{161–180}$ peptide [26]. The line was first fused with the BW5147α^{-}β^{-} cells [27] (a gift from Dr. Joan Goverman, University of Washington) and a hybridoma clone was selected that showed the best growth inhibition upon IRBP$_{161–180}$ peptide stimulation. TCR α and β cDNA sequences were cloned by the 5′ RACE system (Rapid Amplification of cDNA Ends, Invitrogen), and were identified as Trav16 and Trbv5, respectively (NCBI database, http://blast.ncbi.nlm.nih.gov/Blast.cgi). The TCR α and β sequences were placed under control of the promoter and locus control region of the human CD2 gene, and the mouse H-2K promoter, respectively, using previously described plasmids [28,29] (Suppl. Fig. 1C). The TCR α and TCRβ constructs were microinjected together into B10.RIII embryos. Founder mice carrying both TCR genes were bred to B10.RIII wild type (WT) mice and expanded into transgenic lines.

2.3. Flow cytometric analysis

Thymus, spleen, submandibular (eye-draining) lymph nodes, non-draining (inguinal, axillary and brachial) lymph nodes and eyes were isolated to prepare single cell suspensions. Splenic red blood cells were lysed using ACK lysing buffer (Quality Biological, Inc). For analysis of eye-infiltrating cells, enucleated eyes were minced and treated with 10 μg/ml of collagenase D (Roche) for 30 min at 37 °C. Cells were washed and resuspended in culture media for *ex vivo* stimulation (see ahead), or in PBS containing 2% FBS for staining. Fc receptors were blocked using CD16/32 (2.4G2), and the following anti-mouse monoclonal antibodies (mAbs) with various fluorochromes (FITC, PE, PerCP-Cy5.5, PE-Cy7, APC, APC-Cy7, APC Alexa Fluor 780, eFluor 450, Brilliant Violet 421, V500, Brilliant Violet 605) were used: CD4 (RM4-5), CD8α (53-6.7), CD11b (M1/70), CD25 (PC61), CD44 (IM7), CD62L (Mel-14), CD45R/B220 (RA3-6B2), CD49b (DX5), NK1.1 (PK136), Ly-6C/6G (Gr-1), TCRβ (H57-597). The Abs were purchased from BD Bioscience, BioLegend or eBioscience and were used based on the availability of clones and fluorochromes from the respective vendors. Where appropriate, 7-AAD (BD Bioscience) or propidium iodide (PI; Miltenyi Biotech) was used to exclude dead cells. IRBP$_{161–180}$-specific T cells were detected using an IRBP$_{161–180}$-IA^{r}-IgG1 dimer reagent (p161 dimer) [30] after direct conjugation with Alexa Fluor 647 (Invitrogen), or in combination with anti-mouse IgG secondary Ab (FITC or PE-conjugated, BD Bioscience). For analysis of the Vβ repertoire,

lymph node cells were collected and incubated for 20 min at 4 °C with anti-CD16/CD32, anti-TCRβ-APC, CD8α-PE and anti-CD4-PerCP-Cy5.5, and one of the 15 mAbs against TCR Vβx labeled with FITC (BD Bioscience). For intracellular cytokine staining, cells were stimulated in the complete RPMI-10% FBS with 10 ng/ml phorbol myristate acetate (PMA) and 500 ng/ml ionomycin (Calbio-chem) for 4 h in the presence of Brefeldin A (Golgi Plug, BD Biosciences), fixed in 4% paraformaldehyde and permeabilized with Triton buffer (0.5% Triton X-100 and 0.1% BSA in PBS). Abs used for intracellular cytokine staining were the following; anti-mouse IL-4 (11B11), IFN-γ (XMG1.2), and IL-17A (TC11-18H10.1) conjugated with various fluorochromes as described above. Intracellular Foxp3 staining was performed following the manufacturer's protocol (eBioscience). Samples were acquired on a FACSCalibur or a FACSAria (BD Bioscience) and were analyzed using FlowJo software (TreeStar).

2.4. CD4$^+$ T cell purification, sorting, proliferation and cytokine assays

CD4$^+$ T cells were purified from lymph nodes and spleens by passing through a T cell enrichment column (R&D Systems) followed by magnetic negative selection using biotin-conjugated anti-CD8α, CD11b, CD16/32, CD24 (M1/69), B220, CD49b, Ly-6C/6G and NK1.1 mAbs, and streptavidin microbeads (Miltenyi Biotech), or by cell sorting for CD4$^+$ T cells after staining with anti-CD4 mAb and a mixture of FITC-conjugated anti-CD8α, CD11b, CD16/32, CD24, B220, CD49b, Ly-6C/6G and NK1.1 mAbs (dump). In some experiments, naïve CD4$^+$ T cells were sorted into the (FITC-dump)-^{neg}CD4$^+$CD62L^{hi}CD44^{lo} population on the FACSAria cell sorter. For proliferation assays, purified CD4$^+$ T cells (10^5 cells/well) were stimulated for 48–72 h in a 96-well plate with various concentrations of human IRBP$_{161\text{-}180}$ peptide (Anaspec) presented by irradiated (3000 rad) syngenic B10.RIII WT splenocytes (5×10^5 cells/well). Proliferation was determined by [^{3}H]-thymidine incorporation for 12–18 h following 48 h of Ag stimulation. Cytokine levels in the culture supernatant were measured by the Bio-Plex assay (Bio-Rad) and ELISA (R&D) at 48 h, except for IL-2 (24 h).

2.5. Determination of transgene copy numbers by real-time PCR

Genomic DNA was extracted from tail tissue using DNeasy Blood & Tissue Kit (QIAGEN) and nucleotide concentration was measured at A_{260} with ND-1000 NanoDrop spectrophotometer (Thermo Scientific). Custom TaqMan primers and probes were designed for Vrav16 (TCR Vα) and Vrbv5 (TCR Vβ) and for TCRδ as an endogenous control (Applied Biosystems): 161VαF, 5′-CCCGGGACAGTTCTTACTTCTTATT-3′; 161VαR, 5′-TGTAAGAGTCCTGACGAATAAGGAAAAC-3′; 161VαFAM (Reverse), 5′-CCCCACTTGCTGTTTG-3′; 161VβF, 5′-CAGCACTCATGAACACTAAAATTACT-3′; 161VβR 5′-GCTCACATTCCAAAGACTTATTTGCT-3′; 161VβFAM (Forward), 5′-CAGTCACCAAGATATC-3′; TCRδF, 5′-TGCTGTCAAGCTTGGTCAGT-3′; TCRδR; 5′-GTTGTGCTGAACTGAACATGTCA-3′; TC RδFAM (Reverse), 5′-CTGAATTCGAATCTCC-3′. Ten ng of DNA extracted were added to 10 μl TaqMan Universal PCR Master Mix 2×,1 μl primers/probe mix and brought to a final volume of 20 μl with water. The real-time PCR was performed in duplicate using 7500 Real Time PCR System (Applied Biosystems) following a standard protocol: 50 °C for 2 min, 95 °C for 10 min and 45 cycles of 95 °C for 15 s and 60 °C for 1 min. WT DNA that endogenously carries 2 copies of each TCR gene was used as a calibrator. The fold increase of target DNA amount was calculated according to the comparative Ct method ($2^{-\Delta\Delta Ct}$ method), minus the 2 endogenous copies, and transgene copy numbers were calculated using the formula: y (Tg copies) = 2× (fold increase) −2.

2.6. RNA extraction, cDNA synthesis and TCR Vα and Vβ repertoire analysis by real-time PCR

FACS-sorted $CD4^+$ T cells were lysed in 1 ml of TRIzol Reagent (Invitrogen) and stored at −80 °C until RNA extraction using RNeasy extraction kit (QIAGEN). RNA concentration was measured at A_{260} by ND-1000 spectrophotometer. The quality of total RNA was assessed by electrophoresis on a 2% agarose/TBE gel. One μg of RNA was reverse-transcribed to cDNA using Superscript III cDNA synthesis kit with mixture of random hexamer and oligo dT primers (Invitrogen). The TCR Vα and Vβ repertoire was analyzed by real-time PCR using SYBR® Green I. Each reaction mixture contained 4 ng of cDNA, 10 μl Power SYBR Master Mix 2× (Applied Biosystems), 150 nM Cα or Cβ reverse primer and 200 nM of one of the 20 $Vα_x$ [31,32] or 23 $Vβ_x$ family forward primers [33] for the expression of the Vα and Vβ genes (Suppl. Table 1), or 0.5 μM primers for expression of the hypoxanthine phosphoribosyl transferase (HPRT) housekeeping gene; Forward 5′-GTTGGATACAGGCCAGACTTTG-3′, Reverse 5′-GATTCAACTTGCGCTCA TCTTAG-3′. Following the standard PCR cycle as above, a dissociation cycle (15 s at 95 °C, 1 min at 60 °C, 15 s at 95 °C and 15 s at 60 °C) was added to check the dissociation curve and to confirm that only one specific product from each $Vα_x$ and Cα or $Vβ_x$ and Cβ primer combination was amplified. Vα and Vβ expression in peripheral $CD4^+$ T cells from each of the R161 mouse lines was calculated and normalized to their HPRT gene expression and shown as % frequency of the total TCR repertoire detected. As predicted by the sequence alignment of the transgenic TCR cDNA in the database, Trav16d is detected by the combination of Vα17 and Cα primers and Trbv5 is detected by Vβ1 and Cβ primers.

2.7. Adoptive transfer

For the transfer of activated T cells, lymph node cells pooled from peripheral lymph nodes (cervical, submandibular, axillary, brachial and inguinal) were activated *in vitro* with 1 or 2 μg/ml $IRBP_{161–180}$ peptide in DMEM media supplemented with 10% FBS. In some experiments, cells were stimulated under Th1 or Th17 skewing conditions: 10 ng/ml IL-12, 10 μg/ml anti-IL-4 (11B11) with 10 ng/ml IL-2 added on day 2 for Th1, 2.5 ng/ml TGF-β1, 25 ng/ml IL-6, 10 μg/ml anti-IL-4, 10 μg/ml anti-IFN-γ (R4-6A2) with 10 ng/ml IL-23 added on day 2 for Th17 (all recombinant cytokines from R&D). On day 3 activated T cells were harvested and were injected i.p. into syngeneic $RAG2^{-/-}$ recipient mice (1 million per mouse) or WT recipient mice (5 million per mouse). The disease was monitored by fundoscopy starting on day 7, and confirmed by histopathology between day 10 and 14. For transfer of naïve T cells, lymph nodes and spleens were pooled and T cells were enriched with a T cell enrichment column. Naïve T cells were sorted on the FACSAria II for the population of $FITC(dump)^{neg}CD4^+CD62L^{hi}CD44^{lo}$ as described above and 1 million cells were injected i.p into $RAG2^{-/-}$ recipient mice.

2.8. Evaluation of ocular disease

Fundoscopic analysis was performed weekly for detection of clinical signs of retinal inflammation using a binocular fundus microscope. Mice were anesthetized with Ketamine:Xylazine (7:3). Eyes were dilated with drops containing 2.5% Phenylephrine hydrochloride and 0.5% Tropicamide ophthalmic solutions. The fundus was photographed with a Nikon D90 digital camera connected to the Xenon Nova 175 endoscope (KARL STORZ). For histopathology, eyes were enucleated and fixed in 4% glutaraldehyde for 1 h and 10% formaldehyde for additional >24 h, embedded in methacrylate, then processed by H&E staining. Scores were determined according to the criteria for EAU scoring on a scale of 0–4 in half-point increments, based on the number and type of lesions, as described in detail elsewhere [11]. The average score of both eyes from an individual animal was plotted.

2.9. Statistical analysis

Statistical significance for thymic cellularity and % Foxp3$^+$ cells of R161 lines compared to WT, and for histology scores between R161H and R161M was determined by the unpaired *t*-test, and for incidence and clinical scores by 2-way ANOVA using Prism software (GraphPad Software, Inc.).

3. Results

3.1. Cloning of IRBP-specific TCR and generation of TCR Tg (R161) mice

IRBP-specific TCR α and β genes were cloned from a uveitogenic T cell line that had been established and maintained in our laboratory. The line was originally derived from the highly EAU-susceptible B10.RIII mice that had been immunized with the major pathogenic peptide of IRBP, residues 161-180 (SGIPYII-SYLHPGNTILHVD), by repeated stimulations with the $IRBP_{161-180}$ peptide followed by expansion in IL-2-containing medium [26] (Suppl. Fig. 1A, B). The cloned TCR α and β sequences were placed under control of the human CD2 promoter and H-2K promoter, respectively (Suppl. Fig. 1C). Transgenic mice were made directly on the B10.RIII background. Three transgenic lines expressing the same TCR α and β sequences (R161 TCR) were established and were designated R161H, R161M and R161L, based on frequency (high, medium, low) of IRBP-specific T cells detected in these mice, as described ahead.

Although thymic cellularity was comparable between all three lines and their WT littermates, two lines, R161H and R161M, showed a strongly elevated number of single positive (SP) CD4 T cells (Fig. 1A). Since this self-reactive TCR originated from an IRBP-reactive post-thymic T cell that had already undergone positive selection, we hypothesized that this increased number of SP CD4 T cells may reflect efficient thymic positive selection of this IRBP-specific TCR in the Tg mice. To examine this, IRBP-specific T cells were detected in thymus and peripheral lymphoid tissues of all three R161 lines by flow cytometry using an IRBP-specific MHC class II dimer that efficiently detects the $IRBP_{161-180}$-specific TCR (p161 dimer) [30]. The frequencies of IRBP-specific T cells among the SP CD4 T cells varied among three lines: >80% in R161H, 50–60% in R161M, and only 5% in R161L, supporting the notion that repertoire selection in the R161H and R161M thymi was skewed towards positive selection of the R161 TCR (Fig. 1B). The level of expression of the transgenic R161 TCR on the thymocytes as detected by mean fluorescence intensities with p161 dimer staining paralleled the efficiencies of their thymic positive selection (R161H>R161M>R161L) (Fig. 1C). Interestingly, in the peripheral repertoire, the respective frequencies of IRBP-specific cells were substantially lower: ~25% in R161H, <5% in R161M, and only 1–2% in R161L (Fig. 1B). The reason for this reduction may be due to unknown tolerogenic mechanism(s), better survival or more efficient expansion in the periphery of polyclonal T cells bearing endogenously rearranged TCRs.

3.2. R161 mice develop spontaneous uveitis

Because of the higher frequencies of circulating IRBP-specific T cells in the R161 mouse lines, we expected that they would be more prone to developing uveitis. Periodic examination of their ocular phenotype by fundoscopy and histology revealed that two of the three lines, R161H and R161M, developed a high incidence of moderate to severe ocular inflammatory pathology by 2–3 months of age (Fig. 2A, Suppl. Fig. 2). A substantial proportion of the mice showed signs of disease already by 4 weeks of age and progressively reached an incidence of 100% by 12 weeks, with the R161H line preceding the R161M line in incidence and scores (Fig. 2B). The disease scores were confirmed by histology and compared among the R161 lines at the ages between 10 and 16 weeks (Fig. 2C).

Histological characteristics included limbitis, retinitis, choroiditis, and in a proportion of the mice, extensive foci of lymphocytic infiltration and aggregation within the retina (Suppl. Fig. 2B).

On the other hand, R161L mice did not develop significant spontaneous pathology. We only detected minimal to trace disease (up to score 0.5) in fewer than 10% of R161L mice by 3 months of age (Fig. 2A–C). However, injection of CFA, containing 250 μg of mycobacteria in oil, precipitated detectable inflammation in eyes of a substantial proportion of R161L mice (Fig. 2D–F), suggesting that innate environmental stimuli can perturb homeostasis and trigger autoimmune disease in these mice.

3.3. Ocular infiltrating cells display an activated memory phenotype and produce Th1 and Th17 cytokines

To examine the characteristics of ocular infiltrating cells in R161 mice with spontaneous uveitis, we analyzed their ocular inflammatory cell profiles by flow cytometry. The ocular infiltrating cells were composed of monocytes, granulocytes and lymphocytes, including both T cells and B cells (Suppl. Fig. 3). A substantial proportion of $CD4^+$ T cells stained positively with the p161 dimer, particularly in R161H mice (Fig. 3A). However, the dimer staining of eye-infiltrating cells tended to be weaker than that of lymph node cells (compare to Fig. 1B). Because the eye contains the specific antigen, we speculate that the level of TCR expression in cells that have encountered Ag may have been downregulated. Most of the $CD4^+$ T cells displayed an Ag-experienced memory phenotype ($CD62L^{lo}CD44^{hi}$) (Fig. 3B) and contained a high proportion of Th1 and Th17 effector T cells, as evidenced by IFN-γ and IL-17 production in response to an *ex vivo* PMA and ionomycin pulse (Fig. 3C).

In contrast, analysis of peripheral lymph nodes revealed that most eye-draining (submandibular) and non-draining (pooled inguinal, axillary and brachial) lymph node $CD4^+$ T cells had a naïve phenotype ($CD62L^{hi}CD44^{lo}$). In all three R161 lines the submandibular lymph node contained a higher proportion of IRBP-specific T cells than the non-draining lymph nodes (Suppl. Fig. 4), supporting the notion that antigen from the uveitic eye was draining to the submandibular lymph node. While relatively higher frequencies of effector cytokine-producing cells were detected in the eyes of R161H and R161M mice, only a few effector cells were recovered from eyes of R161L mice, which only develop minimal disease. However, irrespective of the disease status, frequencies of cytokine-producing effector $CD4^+$ T cells in submandibular lymph nodes or other non-draining peripheral lymph nodes were comparable across the strains and much lower than in the eyes (Fig. 3C). Given that IRBP-specific cells were fewer in the non-draining lymph nodes (Suppl. Fig. 4), these memory and effector cytokine-producing cells are likely to reflect responses to environmental Ags from skin sites that drain to the peripheral lymph nodes, rather than IRBP-specific responses.

3.4. TCR transgene copy numbers and a skewed repertoire expression contribute to disease

Since the difference in the TCR transgene copy numbers in the three R161 lines can be one of the factors affecting spontaneous disease, we quantitated the transgenic TCR α and TCRβ genes in each R161 line by real-time quantitative PCR (q-PCR). Custom TaqMan primers and probes were designed to detect transgenic Vα and Vβ sequences which are also present endogenously in the WT mice. After normalization to the endogenous TCRδ sequence, copy numbers of TCRα and TCRβ transgenes were calculated by fold increase relative to WT, which carries 2 copies. All three R161 lines showed increased numbers of copies of the target sequences in their genomic DNA, that roughly paralleled the frequencies of the cells

expressing the IRBP-specific TCR and spontaneous uveitis as described above. The results are summarized in Table 1.

Due to integration effects, transgene copy numbers may not be directly proportional to the level of transcription of the transgenic TCR, and may not parallel the level of TCR expression on the cell surface. Because peripheral $CD4^+$ T cells from R161M and especially of R161L mice bound p161 dimer much less efficiently than those of R161H mice despite expressing the same TCR (<5%, Fig. 1B), we examined the TCR repertoire and relative expression of TCR Vα and Vβ mRNA in R161 lines by real-time q-PCR and by flow cytometry (Fig. 4).

The R161 transgenic TCR is detected by Vα17/Cα and Vβ1/Cβ primer combinations (see Materials and methods). Although skewed Vα17 expression was detected in all three R161 lines compared to WT mice, Vβ1 expression by the three lines was less consistent. While Vβ1 was expressed with high frequency in the R161H and R161L lines, the R161M line showed Vβ1 expression not very different from WT mice (Fig. 4A), despite having a detectably higher copy number of the Vβ gene (Table 1). The expression of Vα17 in R161L T cells appeared less prominent than in the other two lines, possibly due to presence of only one copy of the transgenic a chain (Table 1). It is likely that a lower frequency of one or the other chain in R161M and R161L mice may affect the cell surface expression of the assembled TCR on their T cells, compared to that of R161H mice in which V gene segments other than Vα17 and Vβ1 were expressed at relatively lower levels (Fig. 4A).

To evaluate the expression of the functional TCR on the cell surface, the Vβ repertoire of WT and R161 mice was analyzed by costaining of their T cells with anti-CD4 and a commercial panel of Vβ-specific antibodies (Vβ2-14, 17), or the IRBP-specific p161 dimer, as no anti-Vβ1 antibody is commercially available. The frequency of $CD4^+$ T cells that express each individual Vβ TCR is shown in Fig. 4B. $CD4^+$ T cells from R161H and R161L lines, which expressed a high Vβ1 mRNA level by q-PCR, had a repertoire highly restricted to p161 dimer-positive cells (although its expression was low in R161L mice). In contrast, R161M mice, which expressed a low TCR Vβ1 mRNA by q-PCR, had a fairly diverse Vβ repertoire similar to that of WT, but with a higher frequency of p161 dimer-positive cells. We speculate that in R161H and R161L lines, the high expression of Vβ1 as detected by q-PCR constrained the expression of other Vβ chains. Interestingly, cell surface expression of the IRBP-specific TCR did not parallel the level of the TCR mRNA detected by q-PCR, as the R161M line had a higher frequency of dimer-positive cells (Fig. 4B) than would have been predicted by its mRNA expression by q-PCR (Fig. 4A). These data emphasize that it is the level of transgenic TCR expression on the cell surface, detectable by the p161 dimer, and not the level of Vβ1 mRNA or the presence of other Vβ families, that paralleled the kinetics and severity of spontaneous uveitis in the respective lines.

3.5. T cells from R161 mouse lines respond to IRBP peptide and transfer disease

We next examined antigen-specific T cell responses of R161 lines to $IRBP_{161–180}$ peptide *in vitro*. Under non-polarizing conditions, MACS-purified peripheral $CD4^+$ T cells from all three R161 lines, but not from WT mice, proliferated dose-dependently in response to the graded concentrations of $IRBP_{161–180}$ in correlation with the frequency of IRBP-specific T cells in the respective R161 lines (Fig. 5A, left). Antigen-specific IL-2 production in the first 24 h paralleled the proliferative responses (Fig. 5A, right). A panel of proinflammatory cytokines representing the Th1, Th2 and Th17 effector lineages recapitulated the pattern of the proliferative responses of the three lines upon antigen stimulation (Fig. 5B).

To examine the effector phenotype of these IRBP-specific T cells at the single-cell level, their effector cytokine profiles and Foxp3 expression as a marker for regulatory T cells were

examined by intracellular flow cytometry staining after a pulse of PMA and ionomycin. In all three R161 lines, Th1 and Th17 effector phenotypes were readily detectable by their signature cytokine production, IFN-γ or IL-17A, respectively. In contrast, the Th2 phenotype as characterized by IL-4-producing cells was not detected under this condition, although Th2 cytokines were detected by multiplexed ELISA assays in culture supernatants (Fig. 5C). Notably, R161H T cells that had the highest precursor frequency of IRBP-specific T cells by p161 dimer staining appeared to preferentially adopt an effector phenotype, whereas R161L T cells appeared to preferentially adopt the $Foxp3^+$ Treg phenotype (Fig. 5C).

We next performed adoptive transfer experiments of activated or of naïve R161 cells from each of the three lines into naïve $RAG2^{-/-}$ recipients and followed induction of uveitis in the recipients by fundus examination and histopathology. Both *in vitro* activated cells (cytokine profiles as in Fig. 5C, data not shown) and naïve cells (FACS-sorted for $CD62L^{hi}CD44^{lo}$) induced disease in $RAG2^{-/-}$ recipients, with the low-TCR expressing R161L cells being the least potent (Fig. 5D, E). In intact WT recipients, only antigen-activated, but not naïve, R161 cells were uveitogenic: recipients of naïve cells even from the highest transgenic TCR expressing R161H cells remained disease-free for several weeks after transfer (data not shown). This indicates that the ability of naïve R161 cells to induce uveitis in $RAG2^{-/-}$ recipients was dependent on activation by homeostatic expansion in lymphopenic hosts.

3.6. Both Th1 and Th17 cells are pathogenic effectors in R161H mice

Th1 and Th17 cells are both pathogenic effectors in many autoimmune disease models including EAU. To address whether these effector cells are playing pathogenic roles in the spontaneous uveitis model, we adoptively transferred IRBP-specific Th1 or Th17 effector cells into naïve WT recipient mice. Lymphocytes from R161H mice were polarized *in vitro* under non-skewing (Th0), Th1 or Th17 differentiating conditions and examined for Th1 or Th17 phenotypes by intracellular cytokines and transcription factors. While R161H Th0 cells showed no significant skewing, R161H Th1 cells expressed the transcription factor T-bet, a master regulator of Th1, and IFN-γ with >80% frequency. R161H Th17 cells expressed higher levels of the transcription factor RORγt, a master regulator of Th17, and IL-17A with ~60% frequency (Fig. 6A). Both Th1 and Th17 cells were more pathogenic compared to Th0 cells when transferred to naïve recipient mice, and Th1 cells transferred substantially higher disease compared to Th17 cells in this model (Fig. 6B). Thus, pathogenic potential of activated R161H cells is not limited to the lymphopenic environment (Fig. 5E), and Th1 cells may be a dominant effector subset involved in pathogenesis of uveitis in the R161 model.

3.7. Treg cell development and dynamics in R161 TCR Tg mice

Evidence accumulated from previous studies indicates that Treg cells play a critical role in controlling inflammatory responses in autoimmunity. Although the frequencies of $Foxp3^+$ Treg cells in the periphery were comparable among all three R161 lines and were similar to WT mice, $Foxp3^+$ cells in their thymus were reduced. (Fig. 7A). This suggested altered natural Treg (nTreg) selection in the thymus. To further clarify this, we examined the thymus of R161H mice on the $RAG2^{-/-}$ background, in which all T cells express the IRBP-specific TCR. $Foxp3^+$ cells were virtually absent (~0.01% of CD4 single positive) in the thymus of R161H-$RAG2^{-/-}$ mice (Fig. 7B), suggesting that the IRBP-specific $Foxp3^+$ nTreg cells are not positively selected in the thymus and that the $Foxp3^+$ Tregs in thymi of R161 mice on the conventional background must have been cells with endogenously rearranged TCRs. In the periphery of R161H-$RAG2^{-/-}$ mice, however, a small proportion of $CD4^+$ T cells did express Foxp3, and the frequency of $Foxp3^+$ cells increased significantly in the

eyes of these mice. These results suggest that R161 TCR^+ $Foxp3^+$ Tregs can be generated extrathymically (Fig. 7B).

Notably, we detected a higher proportion of $CD4^+$ T cells positive for Foxp3 in uveitic eyes than in the periphery of R161H mice. Although both the total and the IRBP-specific $Foxp3^+$ T cells were enriched in the uveitic eye compared to the draining lymph node, the IRBP-specific cells appeared to have an advantage, in that the p161 dimer-positive population contained a higher proportion of $CD25^+$ cells in the eye than the dimer-negative population, whereas in the draining lymph node the opposite was true (Fig. 7C). Together, these results suggest that the retina-specific R161 TCR-expressing Treg are not selected in the thymus, but can be induced in the periphery, and become enriched within the inflamed target organ.

4. Discussion

We have successfully generated retinal antigen (IRBP)-specific TCR Tg (R161) mice on the uveitis-susceptible B10.RIII background. These mice spontaneously develop ocular inflammatory disease similar to human autoimmune uveitis without the need for active immunization with retinal Ag in adjuvant. The incidence and severity of spontaneous disease appear to be dependent on the expression levels of the retina-specific transgenic TCR, which are affected by transgene copy numbers and integration sites. The early onset around weaning age and the high incidence of disease in two of the three lines generated, R161H and R161M, provides an experimentally viable platform for basic as well as interventional studies, and a valuable source of retina-specific T cells for cellular studies. The chronic-progressive nature of the disease compared to immunization-induced EAU provides a physiologically relevant model for types of uveitis not well represented by the more acute, induced EAU model. Finally, the third line, R161L, in which an innate trigger such as exposure to mycobacteria promotes inflammation in the eye, will provide a platform for unraveling environmental effects on breaking the threshold of resistance to disease, and the transition from homeostasis to pathology.

Multi-parameter analysis of gene copy number *vs.* repertoire diversity, expression of the transgenic TCR on the cell surface and susceptibility to spontaneous uveitis, revealed some plausible correlations and some surprises. While R161H and R161M mice that develop strong disease carried more than 4 copies of both TCR α and TCRβ transgenes, R161L mice that develop minimal or no disease carry only one copy of TCR α with 4 copies of TCRβ. These results support the notion that copy numbers of the transgene directly affect its cell surface expression and consequently the susceptibility to spontaneous uveitis, although the chromosome locus where the transgenes were inserted may also affect expression. As well, high levels of Vβ1 mRNA were correlated with suppressed expression of other Vβ mRNAs. In keeping with this, the most susceptible line, R161H, had a high level of Vβ1 mRNA, high frequency of p161 dimer-binding cells and low expression of other Vβ family members. Surprisingly, however, the R161M line that also developed spontaneous disease with a high incidence, showed a diverse Vβ repertoire with a low frequency of Vβ1 similar to WT. In this line, Vβ1 mRNA expression was the lowest, which may have permitted the expression of endogenous TCRs. This strain had an intermediate frequency of the p161 dimer-binding cells, which was higher than expected from its low Vβ1 mRNA expression, raising the possibility that other Vβs may have combined with Vα17 to form an IRBP-specific TCR. Nevertheless, R161H and R161M mice crossed onto the $RAG2^{-/-}$ background, so that they express only the transgenic TCR, also develop spontaneous uveitis, albeit with slightly lower severity (data not shown), indicating a major contribution of the clonotypic TCR to pathogenesis. Finally, R161L cells expressed relatively high levels of Vβ1 mRNA (possibly accounting for their low Vβ diversity), however, their cell surface Vβ expression was marginal and the frequency of p161 dimer-binding T cells was low, possibly because their

single copy of the TCR α transgene did not provide sufficient expression of TCR α protein to pair with the TCRβ chain, limiting clonotypic TCR expression. This is in line with their low disease susceptibility.

The phenotype of ocular infiltrating $CD4^+$ T cells and the *in vitro* antigen activation results indicate that R161 clonotype can differentiate into either the Th1 or the Th17 lineage, both of which have been associated with disease in other EAU models [34]. Furthermore, R161H T cells that are activated under the Th1 or Th17 polarizing conditions are both pathogenic (particularly Th1), more so than those activated under non-skewing conditions (Fig. 4B). On the other hand, the contribution of Th2 cells in the spontaneous R161 model may be minor, if any, as we only detected secretion of some Th2 cytokines after *in vitro* Ag stimulation, but not from *in vivo* primed cells isolated from eyes or eye-draining lymph nodes. Further studies will be needed to dissect the relative contributions of the different effector subsets to the pathogenesis of spontaneous uveitis.

The R161 clonotype is also able to differentiate to $Foxp3^+$ Treg cells, both *in vitro* and *in vivo*, although it does not appear to be positively selected as natural Tregs in the thymus. For this reason, we believe that the p161 dimer-positive Tregs found in R161 mice are largely induced by contact with retinal antigen. Our data cannot answer the question whether the Treg cells present within the uveitic eyes were induced from conventional Tcells in the periphery prior to entering the eye, or were converted within the eye from conventional (non-Treg) cells. However, enrichment of antigen-specific Treg cells in the uveitic eyes compared to their proportion in the periphery, and even in the eye-draining submandibular lymph node, suggests that they may either be induced directly in the eye, or may proliferate there upon local exposure to retinal antigen. In support of that notion, we and others have presented evidence that antigen presentation and activation of retina-specific T cells can occur in the eye [35,36]. It is intriguing why, despite their presence, inflammation persists. A possible reason could be that the function of Treg cells at the site of inflammation may be inhibited due to presence of inflammatory mediators [37,38]. Interestingly, antigen-specific T cells of the three R161 lines differed in their propensity to convert into Tregs. It remains a question to what extent this might contribute to the distinct course of disease in different R161 lines. An in-depth analysis of these questions is beyond the scope of the current manuscript and is being examined as the subject of another study (Silver, Horai and Caspi, in preparation).

The R161 TCR family of transgenic mice is not the first reported model of spontaneous uveitis. A transgenic mouse for the human MHC class I molecule HLA-A29, which is associated with a type of uveitis known as birdshot retinochoroidopathy, were reported to develop retinal pathology at the posterior pole of the eye [39]. The original strain was lost, but our recent efforts to recreate it have put the contribution of HLA-A29 to spontaneous pathology in this model in question [40]. In an athymic mouse that is grafted with a neonatal rat thymus, the MHC-incompatible thymic tissue fails to efficiently eliminate the high-affinity autoreactive T cells, and results in spontaneous autoimmune disease [41]. Similarly, the deficiency of autoimmune regulator (AIRE) in mice leads to multiorgan autoimmune diseases including uveitis due to the failure of thymic negative selection [42,43]. As mentioned in Introduction, several mouse strains transgenic for HEL as a neo-self Ag under a retina or lens-specific promoter, as well as for the HEL specific 3A9 TCR, also develop spontaneous uveitis [22,23,44]. However, some findings in these mice must be interpreted with caution, because responses may be affected by integration effects, by the level of expression and tissue distribution of the neo-self Ag and by the affinity of the specific TCR, and therefore may be quite different from responses to the native Ag. Thus, the R161 TCR transgenic mice offer some specific advantages over the previously available models that

make them attractive for particular types of studies, e.g., study of natural triggers of uveitis or cell migration, under “amplified” conditions.

In conclusion, TCR transgenic mice specific to native selfantigens are available for only a few autoimmune disease models, namely, type 1 diabetes [13,14], experimental autoimmune gastritis [15,16] and experimental autoimmune encephalomyelitis [17-21]. There is no doubt that they have contributed tremendously to unraveling the basic mechanisms involved in the pathogenesis of the diseases represented by these models. It is of note that some of them develop autoimmune diseases spontaneously under certain environmental conditions (e.g. “dirty” housing) and/or genetic backgrounds (crossed to a specific MHC, or in a lymphopenic situation). Our new model of spontaneous uveitis in R161 TCR Tg mice now joins these other disease models as a valuable tool to study the pathogenesis of potentially blinding uveitic diseases.

Supplementary Material

Refer to Web version on PubMed Central for supplementary material.

Acknowledgments

We thank NEI Genetic Engineering Core for microinjection of TCR transgenic constructs and assistance in maintaining the Tg mouse colonies, NEI Histology Core for processing the slides and NEI Flow Cytometry Core for assistances in cell sorting and analysis. We are grateful to Drs. Hidehiro Yamane and William E. Paul for critical reading of the manuscript. This work was supported by NEI intramural funding, project # EY000184.

Appendix A. Supplementary data

Supplementary data related to this article can be found online at http://dx.doi.org/10.1016/j.jaut.2013.06.003.

Abbreviations

Ag	antigen
IRBP	interphotoreceptor retinoid binding protein
TCR	T cell receptor
CFA	complete Freund’s adjuvant
EAU	experimental autoimmune uveitis
HEL	hen egg lysozyme
RAG	recombination activating gene
WT	wild type
PMA	phorbol myristate acetate
SP	single positive
AIRE	autoimmune regulator

References

[1]. Streilein JW. Ocular immune privilege: the eye takes a dim but practical view of immunity and inflammation. J Leukoc Biol. 2003; 74:179–85. [PubMed: 12885934]

[2]. Caspi RR. Ocular autoimmunity: the price of privilege? Immunol Rev. 2006; 213:23–35. [PubMed: 16972894]

[3]. Nussenblatt, RB.; Whitcup, SM. Uveitis: fundamentals and clinical practice. 3rd ed.. Elsevier; Philadelphia, PA: 2004. Mosby

[4]. Gritz DC, Wong IG. Incidence and prevalence of uveitis in Northern California; the Northern California Epidemiology of Uveitis Study. Ophthalmology. 2004; 111:491–500. [PubMed: 15019324]

[5]. Durrani OM, Meads CA, Murray PI. Uveitis: a potentially blinding disease. Ophthalmologica. 2004; 218:223–36. [PubMed: 15258410]

[6]. Yamamoto JH, Minami M, Inaba G, Masuda K, Mochizuki M. Cellular autoimmunity to retinal specific antigens in patients with Behcet's disease. Br J Ophthalmol. 1993; 77:584–9. [PubMed: 8218058]

[7]. Gery, I.; Nussenblatt, RB.; Chan, CC.; Caspi, RR. Autoimmune diseases of the eye. In: Theophilopoulos, AN.; Bona, CA., editors. The molecular pathology of autoimmune diseases. Taylor and Francis; New York, NY: 2002.

[8]. Descamps FJ, Kangave D, Cauwe B, Martens E, Geboes K, Abu El-Asrar A, et al. Interphotoreceptor retinoid-binding protein as biomarker in systemic autoimmunity with eye inflictions. J Cell Mol Med. 2008; 12:2449–56. [PubMed: 18266969]

[9]. Takeuchi M, Usui Y, Okunuki Y, Zhang L, Ma J, Yamakawa N, et al. Immune responses to interphotoreceptor retinoid-binding protein and S-antigen in Behcet's patients with uveitis. Invest Ophthalmol Vis Sci. 2010; 51:3067–75. [PubMed: 20089879]

[10]. de Smet MD, Yamamoto JH, Mochizuki M, Gery I, Singh VK, Shinohara T, et al. Cellular immune responses of patients with uveitis to retinal antigens and their fragments. Am J Ophthalmol. 1990; 110:135–42. [PubMed: 2378377]

[11]. Horai, R.; Caspi, RR. Animal models for retinal diseases neuromethods. SpringerLink; 2010. Retinal inflammation: uveitis/uveoretinitis; p. 207-25.

[12]. Pennesi G, Mattapallil MJ, Sun SH, Avichezer D, Silver PB, Karabekian Z, et al. A humanized model of experimental autoimmune uveitis in HLA class II transgenic mice. J Clin Invest. 2003; 111:1171–80. [PubMed: 12697736]

[13]. Verdaguer J, Schmidt D, Amrani A, Anderson B, Averill N, Santamaria P. Spontaneous autoimmune diabetes in monoclonal T cell nonobese diabetic mice. J Exp Med. 1997; 186:1663–76. [PubMed: 9362527]

[14]. Verdaguer J, Yoon JW, Anderson B, Averill N, Utsugi T, Park BJ, et al. Acceleration of spontaneous diabetes in TCR-beta-transgenic nonobese diabetic mice by beta-cell cytotoxic CD8+ T cells expressing identical endogenous TCR-alpha chains. J Immunol. 1996; 157:4726–35. [PubMed: 8906855]

[15]. Alderuccio F, Cataldo V, van Driel IR, Gleeson PA, Toh BH. Tolerance and autoimmunity to a gastritogenic peptide in TCR transgenic mice. Int Immunol. 2000; 12:343–52. [PubMed: 10700469]

[16]. McHugh RS, Shevach EM, Margulies DH, Natarajan KA. T cell receptor transgenic model of severe, spontaneous organ-specific autoimmunity. Eur J Immunol. 2001; 31:2094–103. [PubMed: 11449363]

[17]. Goverman J, Woods A, Larson L, Weiner LP, Hood L, Zaller DM. Transgenic mice that express a myelin basic protein-specific T cell receptor develop spontaneous autoimmunity. Cell. 1993; 72:551–60. [PubMed: 7679952]

[18]. Lafaille JJ, Nagashima K, Katsuki M, Tonegawa S. High incidence of spontaneous autoimmune encephalomyelitis in immunodeficient anti-myelin basic protein T cell receptor transgenic mice. Cell. 1994; 78:399–408. [PubMed: 7520367]

[19]. Waldner H, Whitters MJ, Sobel RA, Collins M, Kuchroo VK. Fulminant spontaneous autoimmunity of the central nervous system in mice transgenic for the myelin proteolipid protein-specific T cell receptor. Proc Natl Acad Sci U S A. 2000; 97:3412–7. [PubMed: 10737797]

[20]. Bettelli E, Pagany M, Weiner HL, Linington C, Sobel RA, Kuchroo VK. Myelin oligodendrocyte glycoprotein-specific T cell receptor transgenic mice develop spontaneous autoimmune optic neuritis. J Exp Med. 2003; 197:1073–81. [PubMed: 12732654]

[21]. Pollinger B, Krishnamoorthy G, Berer K, Lassmann H, Bosl MR, Dunn R, et al. Spontaneous relapsing-remitting EAE in the SJL/J mouse: MOG-reactive transgenic T cells recruit endogenous MOG-specific B cells. J Exp Med. 2009; 206:1303–16. [PubMed: 19487416]

[22]. Lambe T, Leung JC, Ferry H, Bouriez-Jones T, Makinen K, Crockford TL, et al. Limited peripheral T cell anergy predisposes to retinal autoimmunity. J Immunol. 2007; 178:4276–83. [PubMed: 17371984]

[23]. Ham DI, Kim SJ, Chen J, Vistica BP, Fariss RN, Lee RS, et al. Central immunotolerance in transgenic mice expressing a foreign antigen under control of the rhodopsin promoter. Invest Ophthalmol Vis Sci. 2004; 45:857–62. [PubMed: 14985302]

[24]. Gregerson DS, Torseth JW, McPherson SW, Roberts JP, Shinohara T, Zack DJ. Retinal expression of a neo-self antigen, beta-galactosidase, is not tolerogenic and creates a target for autoimmune uveoretinitis. J Immunol. 1999; 163:1073–80. [PubMed: 10395707]

[25]. McPherson SW, Heuss ND, Gregerson DS. Lymphopenia-induced proliferation is a potent activator for CD4+ T cell-mediated autoimmune disease in the retina. J Immunol. 2009; 182:969–79. [PubMed: 19124740]

[26]. Silver PB, Rizzo LV, Chan CC, Donoso LA, Wiggert B, Caspi RR. Identification of a major pathogenic epitope in the human IRBP molecule recognized by mice of the H-2r haplotype. Invest Ophthalmol Vis Sci. 1995; 36:946–54. [PubMed: 7706044]

[27]. Letourneur F, Malissen B. Derivation of a T cell hybridoma variant deprived of functional T cell receptor alpha and beta chain transcripts reveals a nonfunctional alpha-mRNA of BW5147 origin. Eur J Immunol. 1989; 19:2269–74. [PubMed: 2558022]

[28]. Zhumabekov T, Corbella P, Tolaini M, Kioussis D. Improved version of a human CD2 minigene based vector for T cell-specific expression in transgenic mice. J Immunol Methods. 1995; 185:133–40. [PubMed: 7665895]

[29]. Pircher H, Mak TW, Lang R, Ballhausen W, Ruedi E, Hengartner H, et al. T cell tolerance to Mlsa encoded antigens in T cell receptor V beta 8.1 chain transgenic mice. EMBO J. 1989; 8:719–27. [PubMed: 2524380]

[30]. Karabekian Z, Lytton SD, Silver PB, Sergeev YV, Schneck JP, Caspi RR. Antigen/MHC class II/Ig dimers for study of uveitogenic T cells: IRBP p161-180 presented by both IA and IE molecules. Invest Ophthalmol Vis Sci. 2005; 46:3769–76. [PubMed: 16186361]

[31]. Casanova JL, Romero P, Widmann C, Kourilsky P, Maryanski JL. T cell receptor genes in a series of class I major histocompatibility complex-restricted cytotoxic T lymphocyte clones specific for a Plasmodium berghei nonapeptide: implications for T cell allelic exclusion and antigen-specific repertoire. J Exp Med. 1991; 174:1371–83. [PubMed: 1836010]

[32]. DiRienzo CG, Murphy GF, Jones SC, Korngold R, Friedman TM. T-cell receptor Valpha spectratype analysis of a CD4-mediated T-cell response against minor histocompatibility antigens involved in severe graft-versus-host disease. Biol Blood Marrow Transplant. 2006; 12:818–27. [PubMed: 16864052]

[33]. Pannetier C, Cochet M, Darche S, Casrouge A, Zoller M, Kourilsky P. The sizes of the CDR3 hypervariable regions of the murine T-cell receptor beta chains vary as a function of the recombined germ-line segments. Proc Natl Acad Sci U S A. 1993; 90:4319–23. [PubMed: 8483950]

[34]. Luger D, Silver PB, Tang J, Cua D, Chen Z, Iwakura Y, et al. Either a Th17 or a Th1 effector response can drive autoimmunity: conditions of disease induction affect dominant effector category. J Exp Med. 2008; 205:799–810. [PubMed: 18391061]

[35]. Lehmann U, Heuss ND, McPherson SW, Roehrich H, Gregerson DS. Dendritic cells are early responders to retinal injury. Neurobiol Dis. 2010; 40:177–84. [PubMed: 20580926]

[36]. Zhou R, Horai R, Silver PB, Mattapallil MJ, Zarate-Blades CR, Chong WP, et al. The living eye “disarms” uncommitted autoreactive T cells by converting them to Foxp3(+) regulatory cells following local antigen recognition. J Immunol. 2012; 188:1742–50. [PubMed: 22238462]

[37]. Valencia X, Stephens G, Goldbach-Mansky R, Wilson M, Shevach EM, Lipsky PE. TNF downmodulates the function of human CD4+CD25hi T-regulatory cells. Blood. 2006; 108:253–61. [PubMed: 16537805]

[38]. Korn T, Reddy J, Gao W, Bettelli E, Awasthi A, Petersen TR, et al. Myelin-specific regulatory T cells accumulate in the CNS but fail to control autoimmune inflammation. Nat Med. 2007; 13:423–31. [PubMed: 17384649]

[39]. Szpak Y, Vieville JC, Tabary T, Naud MC, Chopin M, Edelson C, et al. Spontaneous retinopathy in HLA-A29 transgenic mice. Proc Natl Acad Sci U S A. 2001; 98:2572–6. [PubMed: 11226280]

[40]. Mattapallil MJ, Wawrousek EF, Chan CC, Zhao H, Roychoudhury J, Ferguson TA, et al. The Rd8 mutation of the Crb1 gene is present in vendor lines of C57BL/6N mice and embryonic stem cells, and confounds ocular induced mutant phenotypes. Invest Ophthalmol Vis Sci. 2012; 53:2921–7. [PubMed: 22447858]

[41]. Ichikawa T, Taguchi O, Takahashi T, Ikeda H, Takeuchi M, Tanaka T, et al. Spontaneous development of autoimmune uveoretinitis in nude mice following reconstitution with embryonic rat thymus. Clin Exp Immunol. 1991; 86:112–7. [PubMed: 1914224]

[42]. Anderson MS, Venanzi ES, Klein L, Chen Z, Berzins SP, Turley SJ, et al. Projection of an immunological self shadow within the thymus by the aire protein. Science. 2002; 298:1395–401. [PubMed: 12376594]

[43]. DeVoss J, Hou Y, Johannes K, Lu W, Liou GI, Rinn J, et al. Spontaneous autoimmunity prevented by thymic expression of a single self-antigen. J Exp Med. 2006; 203:2727–35. [PubMed: 17116738]

[44]. Zhang M, Vacchio MS, Vistica BP, Lesage S, Egwuagu CE, Yu CR, et al. T cell tolerance to a neo-self antigen expressed by thymic epithelial cells: the soluble form is more effective than the membrane-bound form. J Immunol. 2003; 170:3954–62. [PubMed: 12682222]

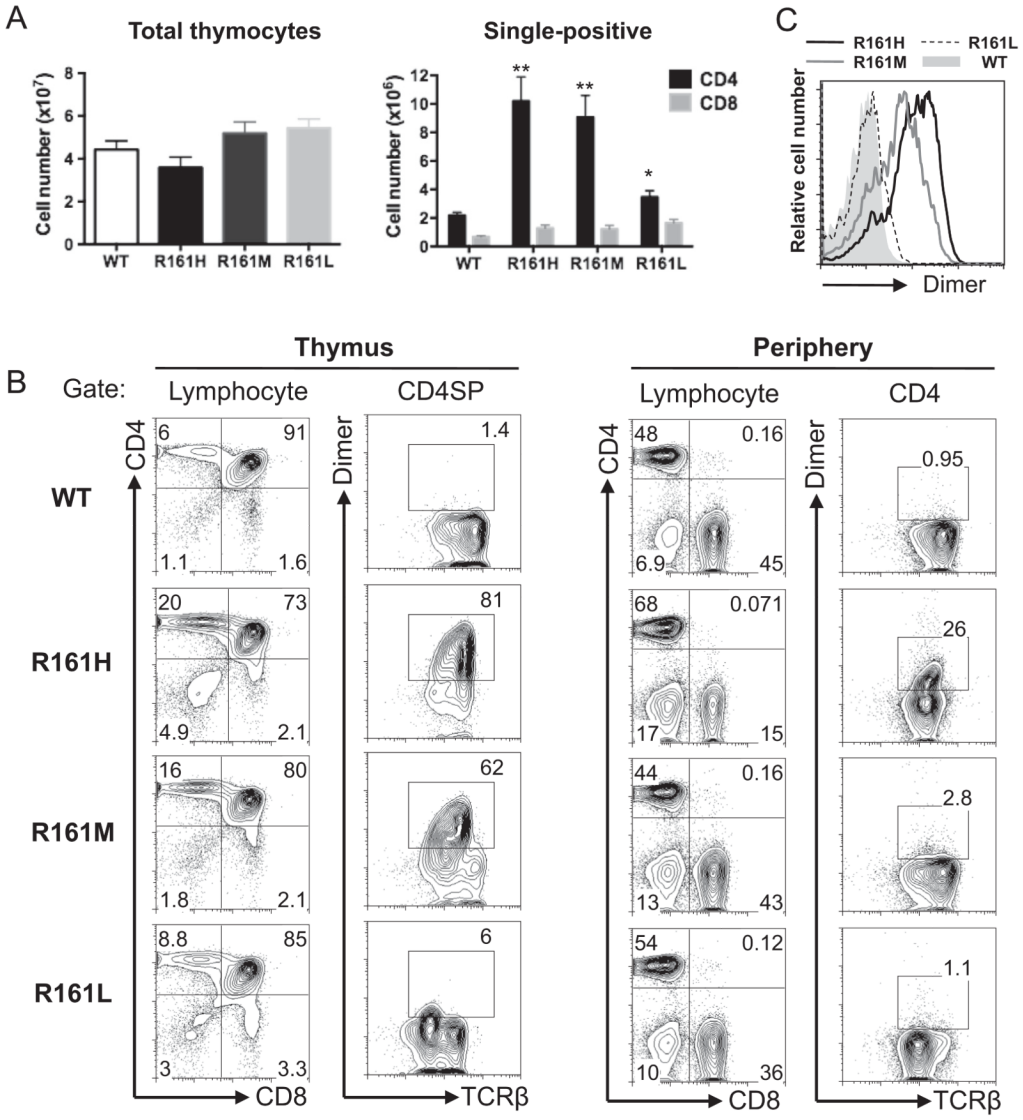

Fig. 1.

Generation of IRBP-specific TCR transgenic (R161) mice. A. Total thymocyte and CD4/CD8 single positive (SP) cell counts (mean ± SEM) in WT and R161 lines between 8 and 15 weeks of age. The data was averaged from several experiments using total of 7–12 mice in each Tg line. $^{**}p < 0.001$, $^{*}p < 0.05$. No significance was detected in total thymocyte or CD8 SP numbers of R161 lines compared to that of WT. B. Lymphocyte profiles of thymus (left) and peripheral T cells (right) of WT and R161 lines. IRBP-specific T cells were detected within the $CD4^+$ population by the $IRBP_{161\text{-}180}/IA^r$-Ig dimer reagent (Dimer) and TCRβ expression as gated. C. The expression levels of IRBP-specific TCR (Dimer-binding) in the thymus CD4 SP population were overlaid and compared between R161 lines in the histograms. The data is representative of at least 3 experiments using 2–3 mice per line.

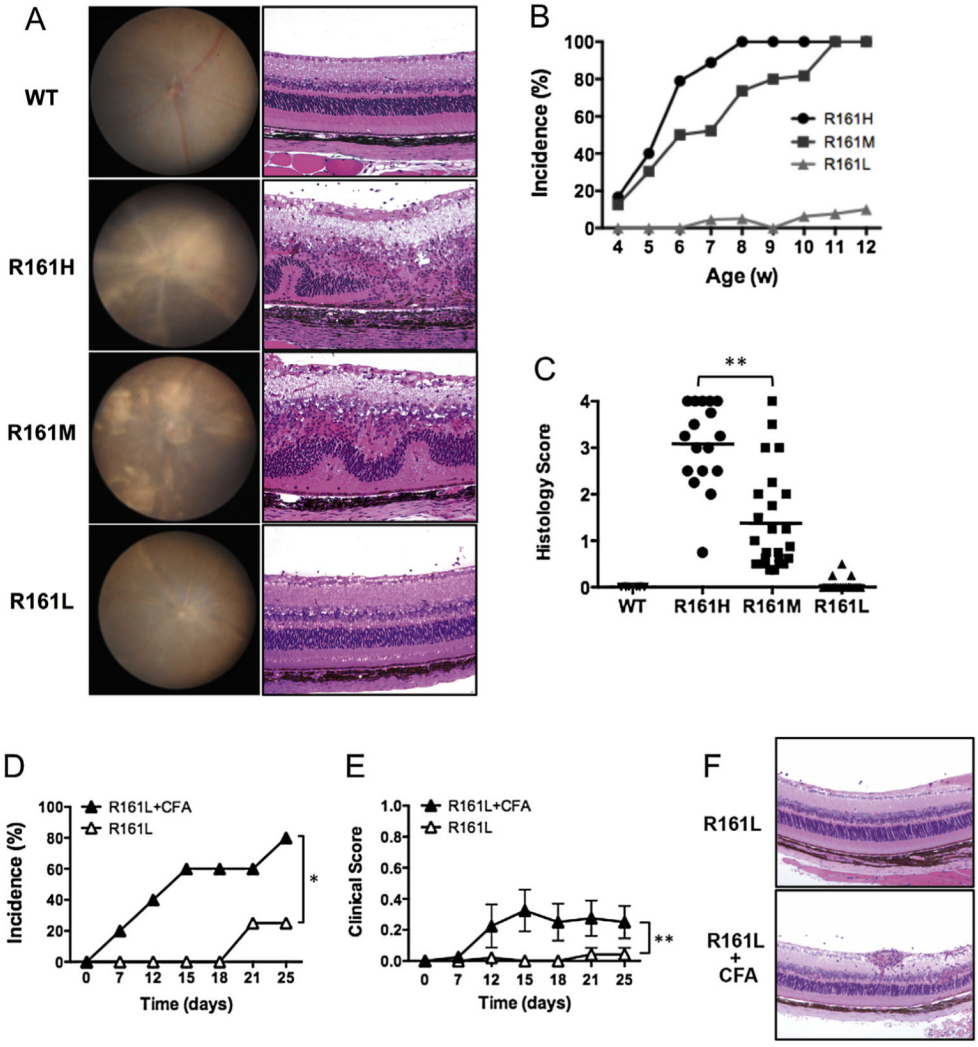

Fig. 2.

Development of spontaneous uveitis in R161 lines. A. Fundus images (left) and histology pictures of retina (right, original mag. ×200) of R161 lines. WT shows normal fundus and histology. R161H and R161M show moderate to severe inflammatory lesions e.g. retinitis and choroiditis (see Suppl. Fig. 2 for detailed histopathology of R161H), whereas R161L shows mild lesions with few cellular infiltrates in the vitreous. B. Incidence of spontaneous uveitis determined by weekly fundus examination. Numbers of mice evaluated per time points; R161H ($N = 11–40$), R161M ($N = 15–24$), R161L ($N10–22$). C. Individual histology scores (symbols) and the average (line) evaluated by histology between 8 and 16 weeks of age. $^{**}p < 0.0001$ by unpaired t-test. D–F. R161L mice ($N = 5$) were injected s.c. with 0.2 ml CFA (containing 250 ug M. tuberculosis). Shown is disease incidence (D) and clinical score (E) by fundus examination compared to age-matched R161L littermates without injection ($N = 6$). $^{*}p < 0.05$ and $^{**}p < 0.0001$ by 2-way ANOVA. F. Histology picture of R161L retina at day 25 post-injection of CFA and its control.

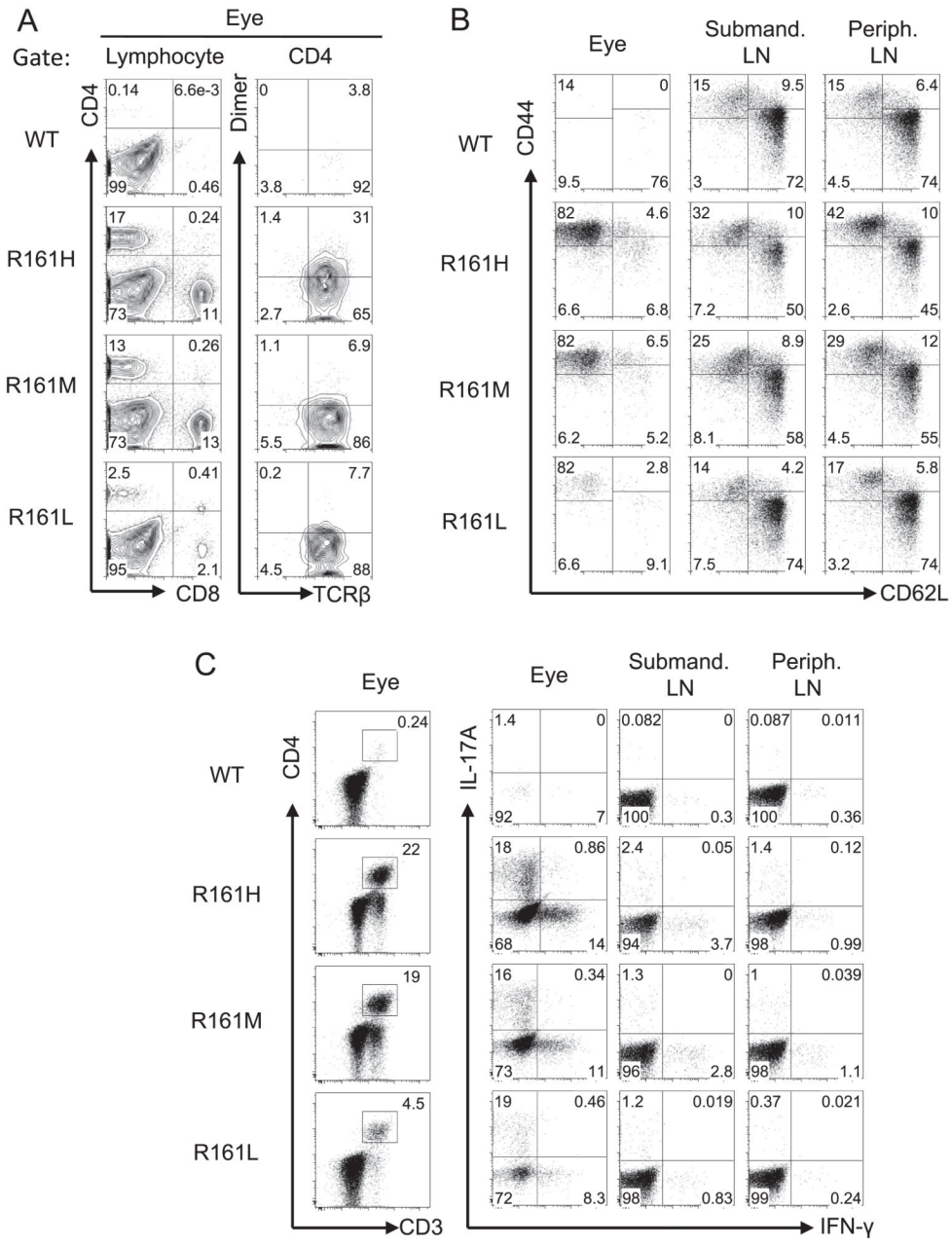

Fig. 3.

Ocular infiltrating lymphocytes display an activated/memory phenotype in R161 lines. A. Infiltrating lymphocytes in uveitic eyes included $CD4^+$ and $CD8^+$ T cells in all R161 lines. Substantial proportions of these $CD4^+$ T cells expressed IRBP-specific TCRs. B. Naïve ($CD62L^{hi}CD44^{lo}$) and memory ($CD62L^{lo}CD44^{hi}$) profiles of eye-infiltrating $CD4^+$ T cells and lymph node (LN) $CD4^+$ T cells. C. CD3/CD4 profiles (left) and IFN-γ and IL-17A production (right) from eye-infiltrating cells and LN cells following *ex vivo* PMA and ionomycin stimulation in the presence of Brefeldin A. CD3/CD4 plots are gated on lymphocytes by size and IFN-γ/IL-17A plots are gated on $CD3^+CD4^+CD8^-$ T cells. Peripheral (non-draining) LN are pooled inguinal, axillary and brachial LN.

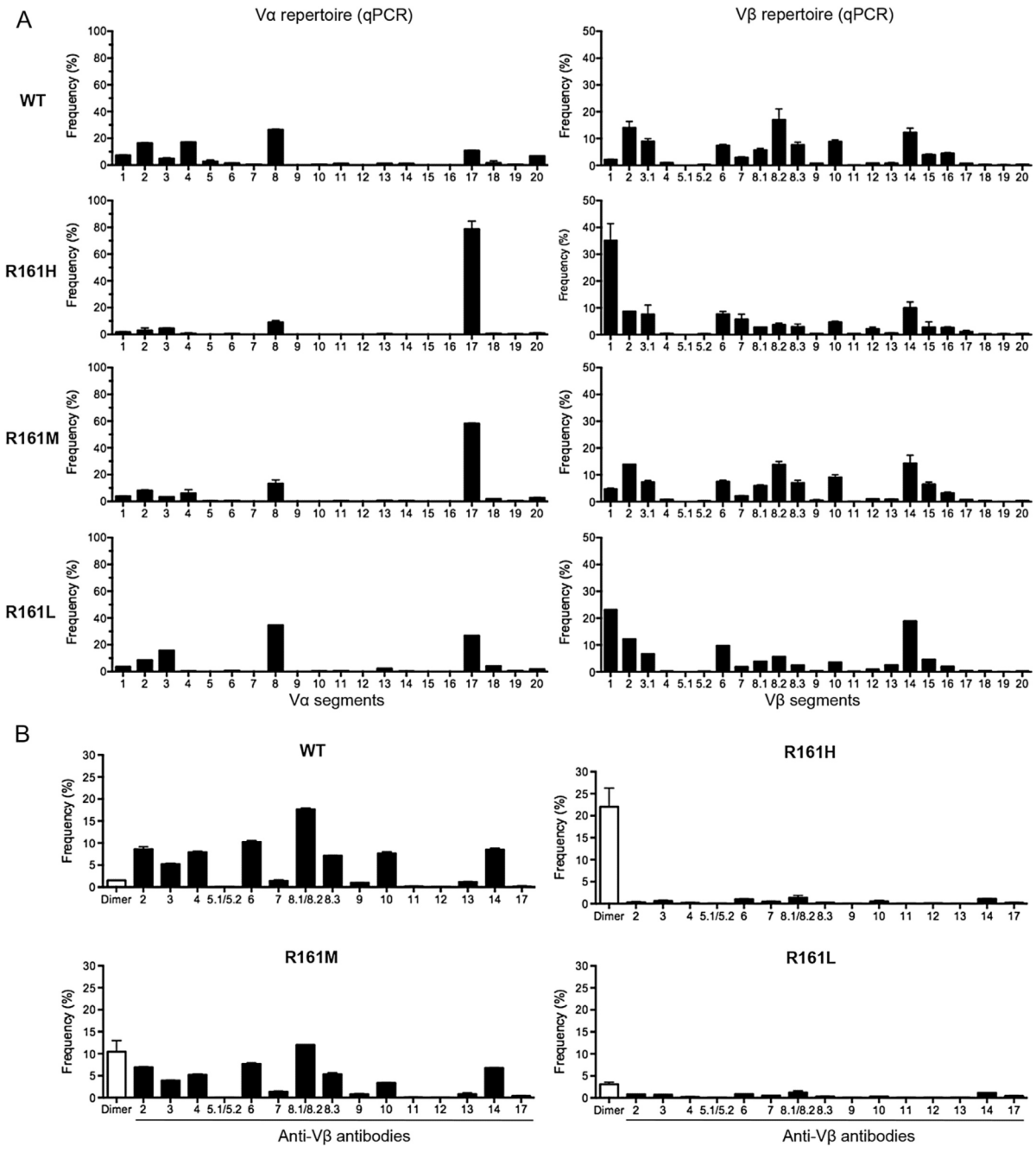

Fig. 4.

Skewed TCR repertoire in R161 mouse lines. A. Vα and Vβ TCR repertoire. $CD4^+$ T cells were sorted from lymph nodes and each Vα and Vβ TCR mRNA expression was measured by real-time quantitative PCR (q-PCR). Relative frequency of each Vα or Vβ TCR was calculated as described in Materials and methods. B. Cell surface Vβ expression analysis by flow cytometry with indicated anti-Vβ mAbs (black bars, Vβ2-14, 17) or with IRBP-specific dimer (Dimer) that binds to transgenic TCR (white bar). Frequency (%) was determined in the $CD4^+$ gate.

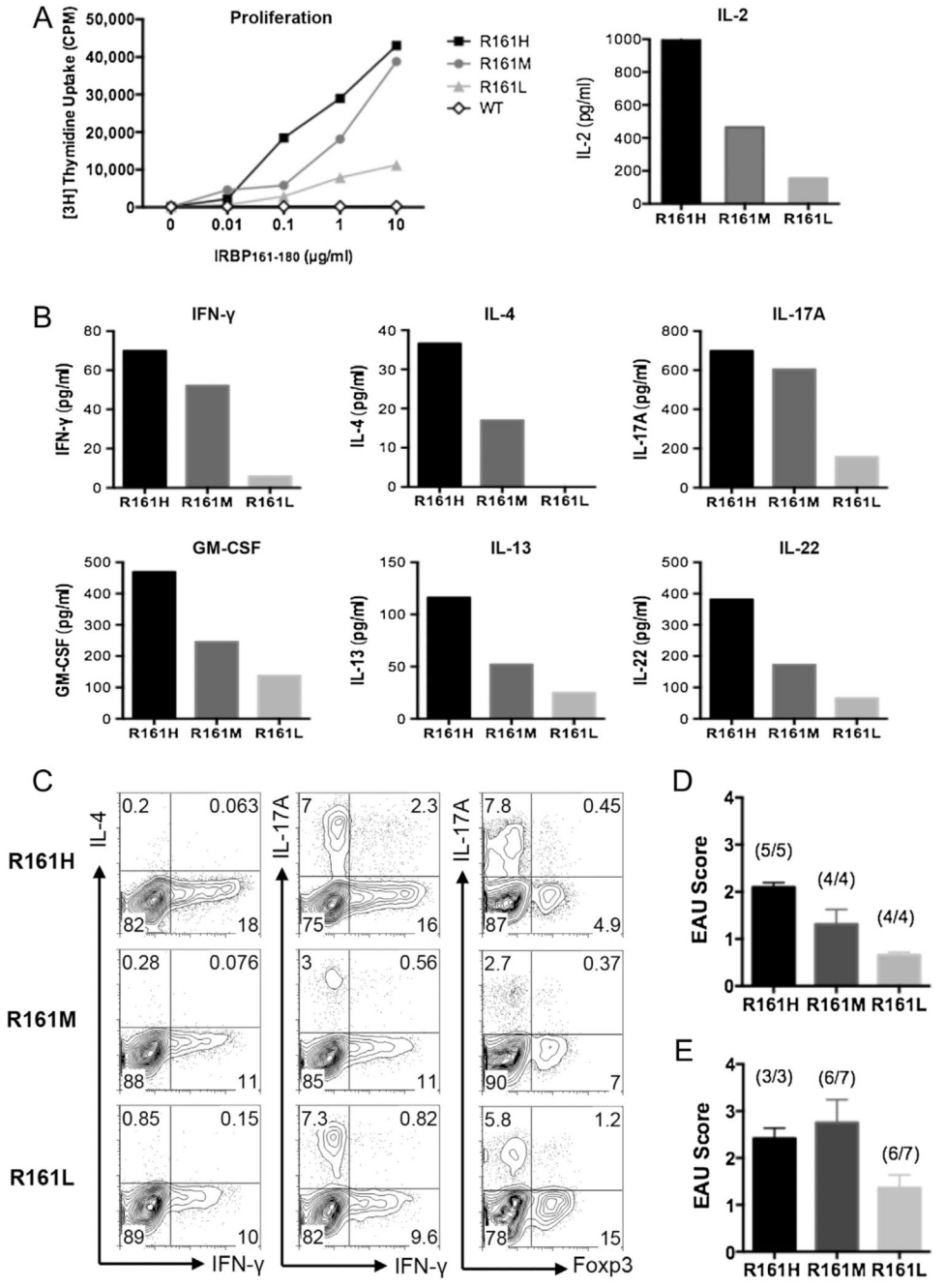

Fig. 5.

Antigen-specific responses of R161 $CD4^+$ T cells. A. Left: Proliferation of purified peripheral $CD4^+$ T cells from R161 lines to various concentrations of specific Ag $IRBP_{161–180}$ in the presence of irradiated (3000 rad) splenic APC from syngeneic WT mice. Right: IL-2 secretion at 24 h stimulation with 1 μg/ml $IRBP_{161–180}$ peptide. B. Inflammatory cytokine secretion in the culture supernatant at 48 h stimulation with 1μg/ml $IRBP_{161–180}$ peptide. Data is representative of at least 3 independent experiments. WT supernatant did not contain detectable cytokines. C. Flow cytometric intracellular cytokine analysis of *in vitro* activated R161 lymph node T cells with 1μg/ml $IRBP_{161-180}$ peptide at 72 h followed by PMA and ionomycin pulse in the presence of Brefeldin A. D. Adoptive

transfer of 1×10^6 *in vitro* activated R161 T cells into B10.RIII-RAG2$^{-/-}$ recipients. EAU was evaluated by histopathology at day 10 of the transfer. E. Adoptive transfer of 1×10^6 sorted naïve (CD62L^{hi}CD44^{lo}) R161 CD4$^+$ T cells into B10.RIII-RAG2$^{-/-}$ recipients. EAU was evaluated by histopathology on day 12 (R161H) or day 14 (R161M, L) after adoptive transfer. The incidence (number of mice develop disease/total mice) is indicated above the bar of each group.

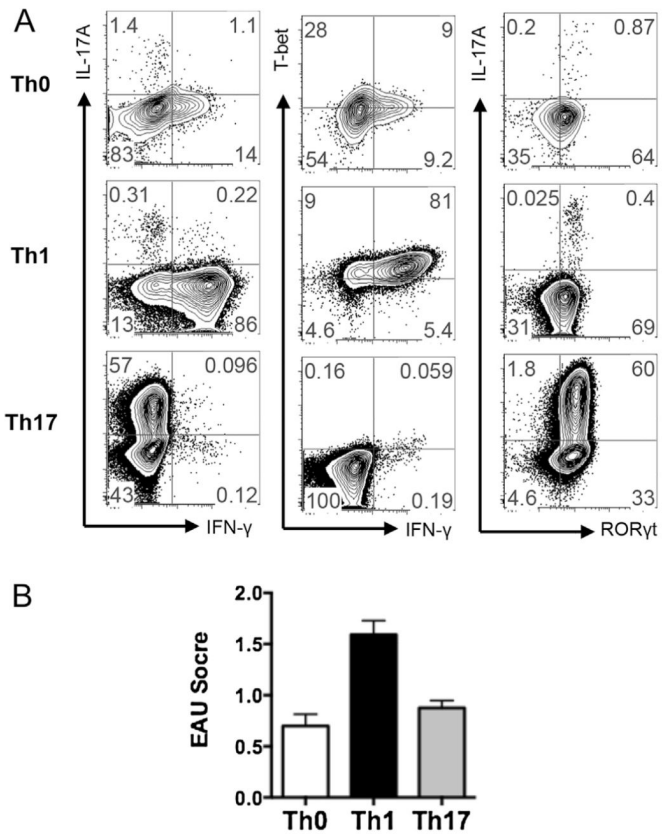

Fig. 6.

Th0, Th1 and Th17 R161H TCR Tg cells are all pathogenic in naïve recipients. A. Polarization of R161H T cells in non-skewing (Th0), Th1 or Th17 conditions. Total lymph node cells were stimulated with 1μg/ml $IRBP_{161–180}$ for 3 days. B. Adoptive transfer of Th0, Th1 and Th17 cells in WT recipient mice. Eyes were collected for EAU scoring by histopathology on day 11–14 of the transfers. Shown are pooled data from 4 independent experiments for Th0 and 2 independent experiments for Th1 and Th17 conditions.

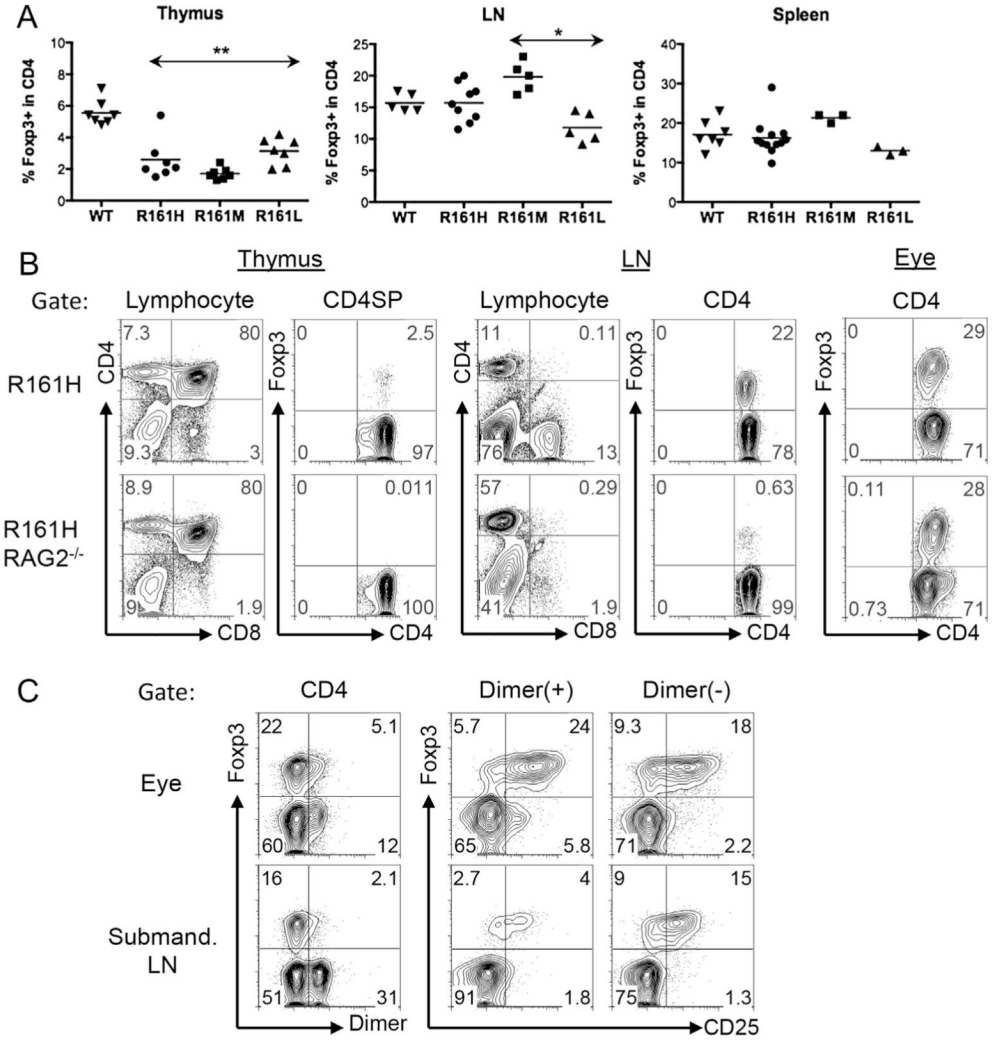

Fig. 7.

Foxp3 expression in the thymus, lymphoid tissues and uveitic eyes of R161 mice. A. Percent of Foxp3$^+$ cells in the CD4 population in the thymus, lymph nodes and spleen from WT and R161 mice was determined by flow cytometry. $^{**}p < 0.005$, $^{*}p < 0.05$ compared to WT. B. R161H mice on the RAG2$^{-/-}$ background do not develop Foxp3$^+$ Treg cells in the thymus. C. Uveitic eyes of R161H contain Foxp3$^+$ Treg cells, including IRBP-specific Tregs.

Table 1

TCR α and β transgene copy numbers determined by q-PCR.

Lines	*N*	Fold increase over WT		Calculated transgene copies	
		Vα	Vβ	Vα	Vβ
WT	7	1	1	0	0
R161H	18	3.5	5	5	8
R161M	6	4	3	6	4
R161L	6	1.5	3	1	4

Data were obtained from multiple assays by averaging the fold increase over WT samples in each q-PCR reaction. N, number of mice analyzed from each line.